JACS
JOURNAL OF THE AMERICAN CHEMICAL SOCIETY
Article
pubs.acs.org/JACS

Zeolite Synthesis in Fluoride Media: Structure Direction toward ITW by Small Methylimidazolium Cations

Alex Rojas,[†] Evangelina Martínez-Morales,[‡] Claudio M. Zicovich-Wilson,[‡] and Miguel A. Camblor*[,†]

[†]Instituto de Ciencia de Materiales de Madrid, ICMM-CSIC, Sor Juana Inés de la Cruz 3, 28049 Madrid, Spain

[‡]Facultad de Ciencias, Universidad Autónoma del Estado de Morelos, Av. Universidad 1001, Col. Chamilpa, 62209 Cuernavaca (Morelos), Mexico

Supporting Information

ABSTRACT: Pure silica ITW zeolite can be synthesized using 1,2,3-trimethylimidazolium and 1,3-dimethylimidazolium cations and fluoride anions as structure-directing agents (SDAs). Similarly to the previously reported 1,3,4-trimethylimidazolium, the dimethyl cation can also produce the zeolite TON, but this higher framework density phase finally transforms *in situ* into ITW. The structures of the as-made and calcined phases prepared with the new cations show a unit cell doubling along *z*, and the refined structures are reported. Periodic Density Functional Theory calculations provide the energies of the six SDA-ITW and SDA-TON zeolites, and their relative stabilities fully agree with the experimental observations. Structure-direction in this system is discussed from experimental and theoretical results that give strong support to the idea that strained silica frameworks are made possible in fluoride media by decreasing the covalent character of the Si−O bond. This decreased covalency is enhanced with the 1,2,3-trimethyl isomer, which is shown to be the strongest SDA for ITW and, at the same time, is the more hydrophilic of the three SDAs tested. Our observations with the three SDAs agree with the so-called Villaescusa's rule, i.e., the low framework density phase is favored at higher concentrations, but at the same time question the supersaturation hypothesis that has been proposed to explain this rule, since here the low-density phase is the most stable one.

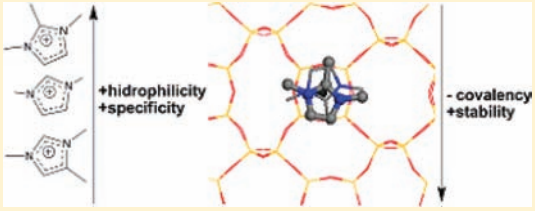

INTRODUCTION

Structure-direction, i.e., the ability to select a particular phase among many possible, is a key issue in the synthesis of zeolites. Despite the high pace at which new Zeolite Framework Type Codes (FTCs)[1] are recognized by the International Zeolite Association (averaging almost seven new types per year for the past 14 years), there is still little understanding, at a molecular level, of what determines the phase that actually crystallizes. In support to this statement, the *a priori* design of zeolites still remains largely a goal: apparently, most new materials are discovered by trial and error, even if the attempts are somehow guided[2] by the empirical knowledge accumulated over the past half-century and the attempts to rationalize it.[3−5]

Pure silica zeolites appear to be metastable with respect to quartz, with their energies increasing as their density decreases.[6] Nonetheless, for known phases the energy penalty associated with porosity is small, and we have recently shown that it is indeed possible to transform *in situ* in the crystallizing medium a zeolite (Framework Type Code TON, with a framework density (FD, number of Si tetrahedra per nm^3) of 19.75 Si/nm^3) into another one of lower framework density (ITW, FD = 18.09 Si/nm^3).[7] This is despite the fact that our Density Functional Theory (DFT) calculations evidenced an energy difference between both zeolites (in their clean, i.e., calcined, SiO_2 form) that is larger than expected from their difference in density, due to the strained double four-member-ring units (D4R) found in the lower density phase. The transformation is mediated by a relatively large stabilization energy provided by the ionic guests used as "structure-directing agents" (SDAs): the fluoride anion and the 1,3,4-trimethylimidazolium cation (134TMI) (see Chart 1). One of the key factors affording the transformation is the increased ionization of the ITW SiO_2 framework by interaction with its ionic guests: with more ionic, less oriented, Si−O bonds the structural strain associated to unfavorable Si−O−Si angles is reduced.

Chart 1. Organic Cations Used in This Work

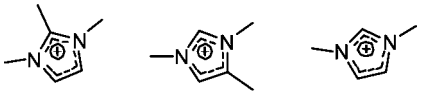

Here we report our work with two additional imidazolium cations that afford the crystallization of ITW: 1,2,3-trimethylimidazolium (123TMI) and 1,3-dimethylimidazolium (13DMI) (Chart 1). Depending on the synthesis conditions, the smallest of these SDAs (13DMI) allows the same TON→ITW high-to-low density transformation previously reported. By contrast, 123TMI, which is an isomer of the previously reported 134TMI,[8] appears to be extremely selective for pure

Received: October 19, 2011
Published: January 4, 2012

   dx.doi.org/10.1021/ja209832y | J. Am. Chem.Soc. 2012, 134, 2255−2263

silica ITW. Our periodic DFT calculations for the two SiO_2 phases and the three organic SDAs agree well with the experimental observations. The ITW zeolites prepared with the SDAs reported here show additional reflections revealing a doubling of the cell previously reported, which is now clearly detected due to preferred orientation effects.

EXPERIMENTAL SECTION

Synthesis of the Organic Cations. The organic cations used in this work (Chart 1) were synthesized by methylation or double methylation at N positions of the appropriately substituted imidazoles. The synthesis of 134TMI was done as previously reported.[8] For the other cations, the following recipes were used.

1,2,3-Trimethylimidazolium Iodide (123TMII). First, 8.0 g of 1,2-dimethylimidazole (Aldrich, 98%) was disolved in 100 mL of chloroform (Aldrich, 99%). The solution obtained was mixed with an excess (9 mL) of iodomethane (Aldrich, 99%) and kept under magnetic stirring at room temperature for 2 days. The resulting solid was separated from the solvent by rotary evaporation under a vacuum at 80 °C. (***Caution!*** *Toxic vapors evolve. Use a trap and work under a fume hood.*)

1,3-Dimethylimidazolium Iodide (13DMII). First, 8.3 g of 1-methylimidazole (Aldrich, 99%) was disolved in 100 mL of chloroform (Aldrich, 99%). An excess (9 mL) of iodomethane (Aldrich, 99%) was then added, and the mixture was stirred at room temperature for 2 days. The solvent was removed by rotary evaporation under a vacuum at 70 °C. (***Caution!*** *Toxic vapors evolve. Use a trap and work under a fume hood.*)

Prior to their use, all the iodide salts were converted to the hydroxide form by anion exchange using Dowex monosphere 550A (OH) anion-exchange resin. The hydroxide solutions were concentrated by rotary evaporation to around 1−1.5 mol/1000 g. The final hydroxide concentration was determined by titration using phenolphthalein as indicator, and the solutions were discarded if the total amount of hydroxide obtained was lower than 90% of the starting iodide. This is to prevent spurious results in case of extensive degradation of the organic cation.

As a way to characterize the hydrophobicity of the three imidazolium SDAs, the phase-transfer behavior of their iodide forms from water to chloroform has been measured following an experimental procedure previously reported by Kubota et al.[9]

Zeolite Synthesis. For the zeolite synthesis, tetraethylorthosilicate was hydrolyzed under magnetic stirring at room temperature in an aqueous solution of the hydroxide form of the corresponding organic cation. All the ethanol produced by the hydrolysis, and some water, was allowed to evaporate, and stirring was stopped when the desired composition was achieved. The amount of water evaporated was monitored by weight. Finally, HF (ca. 48% Aldrich, recently titrated) was added while stirring with a spatula for 15 min. The crystallization was carried out at 150 °C in Teflon vessels inside stainless steel autoclaves that were tumbled at about 60 rpm. At different intervals of time, the autoclaves were taken out from the oven, and the solid product was recovered, washed with ample amounts of water, and dried at 100 °C. The final composition of the reaction mixtures was SiO_2:0.5SDAOH:0.5HF:$x$$H_2O$, and the water-to-silica ratio, x, varied between 6 and 25.

Characterization. The recovered solids were identified by power X-ray diffraction (XRD) recorded with a Bruker D8 Advance diffractometer using Cu Kα radiation (λ = 1.5418 Å), in the 2θ range from 5° to 45°. Multinuclear magic angle spinning nuclear magnetic resonance (^{19}F, ^{13}C, ^{29}Si MAS NMR) spectra were recorded on a Bruker AV 400WB; details are given in the Supporting Information. Thermogravimetric analyses were performed under oxygen flow (100 mL/min) in SDT Q600 TA Instruments equipment up to 1000 °C (heating rate 10 °C/min). CHN analyses were carried out in a LECO CHNS-932 instrument.

Rietveld Refinement. The structures of as-made and calcined ITW samples prepared using 123TMI were refined against powder XRD data recorded at the 8C2 beamline at Pohang Acceleration Laboratory (Pohang, Korea) using monochromatic synchrotron radiation (λ = 1.5500 Å). The structure of as-made 13DMI-ITW was refined against powder XRD data recorded in a conventional Philips X'Pert diffractometer with monochromatized Cu Kα_1 radiation (λ = 1.5406 Å). Details of data collection and refinement are given in the Supporting Information.

Theoretical Calculations. All *ab initio* calculations have been realized adopting the periodic approximation at the B3LYP[10,11] (hybrid density functional) level of theory as implemented in the CRYSTAL09 code.[12] Geometry optimizations have been performed employing gradient methods. Both atomic position and cell parameter components of the gradient have been computed analytically. The basis set considered was a VDZ with polarization on Si, O, and F, previously employed in refs 7 and 13. The tolerances for computation of the infinite series involved in energy calculations were those recommended in the code manual.[12] The exchange-correlation functional was numerically integrated by adopting standard tolerances and a (75,438)p grid (see keyword LGRID in the code manual).[12] These conditions allow for an accurate enough evaluation of the geometries, vibrational properties, and relative energies for the present family of systems.

The Born dynamical charge for each atom has been computed as the average diagonal value of the tensor containing the derivatives of the total dipole moment with respect to the corresponding atomic coordinates.[12]

RESULTS AND DISCUSSION

Zeolite Synthesis. We have screened a range of water/silica ratios and crystallization times at 150 °C under rotation for the synthesis of silica zeolites using the three SDAs depicted in Chart 1. The results are summarized in Table 1 and show that 123TMI is the best-performing SDA, in terms of specificity and velocity of crystallization, for the synthesis of ITW, among

Table 1. Results for the Synthesis of Pure Silica Zeolites Using the Three Imidazoliums of Chart 1 at Varying Concentrations

SDA	H_2O/SiO_2	time (days)	product[a]
123TMI	24.5	5	ITW
		9	ITW
		14	ITW
	15.5	5	ITW
		14	ITW
	6.5	3	ITW
		7	ITW
		15	ITW
134TMI	15.5	7	TON
		9	TON + dense
		14	dense
	6.5	3	TON + ITW + amorphous
		7	ITW
		15	ITW
13DMI	24.5	5	amorphous
		14	dense
	15.5	5	TON
		9	TON
		14	TON + dense
	6.1	3	ITW
		7	ITW
		17	ITW

[a]By XRD. "Dense" refers to a phase with an XRD pattern similar to that of tridymite.

dx.doi.org/10.1021/ja209832y | J. Am. Chem.Soc. 2012, 134, 2255−2263

the three tested: with this SDA not only is the crystallization considerably faster, but also ITW is the only crystalline phase observed in a wide range of water/silica ratios (6.5−24.5) and crystallization times (3−14 days).

By contrast, the syntheses of ITW with the originally reported 134TMI[14] and with the newly tested 13DMI show a much reduced crystallization field with regard to water/silica ratio and crystallization time. With these two SDAs the empirical observation summarized in what has been recently[15] termed Villaescusa's rule holds: phases with lower framework density are favored at lower water/silica ratios (higher concentration).[16] This rule has not been convincingly rationalized yet but apparently is the typical observation for the synthesis of zeolites through the fluoride route.[17] Peculiar to our present results is that in this case Villaescusa's rule holds even if the as-made low FD phase (ITW) is thermodynamically more stable than the as-made high FD phase (TON).[7] Thus, while up to now the typical observation was that, in cases where phase transformations were observed, the transformation was from the phase favored at high concentration to the one favored at low concentration, in this case the transformation is from the phase favored at low concentration to the one favored at high concentration. This is, in our view, an important finding regarding Villaescusa's rule because previously it was argued that a high concentration implies a more supersaturated medium that would favor metastable phases, while at low concentration the more thermodynamically stable phase would be favored.[16] In addition to the difficulty in determining supersaturation levels under synthesis conditions, this explanation is questioned by our results, at least for the system under study here, which follows Villaescusa's rule but contradicts the supersaturation hypothesis outlined above: at high concentration the phase with lower framework density but thermodynamically more stable is still preferred.

The synthesis of ITW with 123TMI and 13DMI in fluoride medium contrast with the results previously reported using hydroxide as a mineralizer, where these SDAs have been shown to be highly selective to MTW (containing large-pore 1D channels) and TON (medium-pore 1D channels) zeolites, respectively.[18] Indeed, in the syntheses of high-silica zeolites in hydroxide media, a variety of imidazolium derivatives used as SDAs were found to direct the crystallization preferentially toward "zeolites with parallel one-dimensional pore systems" containing few or no 4MR.[19] By contrast, ITW has a large density of 4MR in the form of D4R, and its pore system is better described as an arrangement of slit-shaped $[4^4 5^4 6^4 8^4]$ cages connected through 8MR pores running in two dimensions. This difference in phase selectivity of 123TMI and 13DMI in fluoride and hydroxide media is likely related to a "structure-direction" effect of fluoride toward zeolites containing 4MR and D4R. Such an effect was proposed long ago[20,21] but lacked a convincing rationale until very recently, when charge-transfer effects in ITW were shown to ionize the Si−O bond, affording relaxation of an otherwise strained structure, making it reachable for crystallization[13] (and even making it more stable that the competing TON zeolite).[7] Also in contrast to our results, 13DMI has been reported to yield only TON zeolite in fluoride medium at 150 °C in static conditions across a range of water/silica ratios (3.5−14.5) similar to that used by us.[22] While this difference may likely be a consequence of the static synthesis, the lack of information on crystallization time and gel composition in ref 22 impedes a proper comparison.

Another important point derived from the results in Table 1 is that our previous finding of a TON-to-ITW transformation[7] is not an extremely rare event subject to very specific conditions: it occurs not only for 134TMI but also for 13DMI and not only in static conditions at high temperature (175 °C)[7] but also under rotation at the lower temperature of 150 °C, i.e, in conditions rather typical for the synthesis of pure silica zeolites.

When the syntheses using 134TMI and 13DMI are compared, it can be concluded that they perform quite similarly, although 13DMI may perform slightly better as an SDA for the synthesis of ITW. Qualitatively the performance of the three imidazolium cations in directing the crystallization toward ITW can be summarized as 123TMI ≫ 13DMI ≳ 134TMI.

It is typically believed that the performance of an SDA may depend on its size, shape, conformational rigidity and "hydrophobicity".[3,4,9,23] Since 123TMI and 134TMI are isomers and have about the same molecular volume and conformational rigidity (restricted to the rotation of the methyl groups around their C−C or C−N bonds), their different behavior may point to their different shape or to more subtle chemical differences. We have measured the transfer from water to chloroform for the three imidazolium SDAs in iodide form, which has been considered a good way to discriminate differences in hydrophobicity, which in turn has been related to their behavior as SDAs in the synthesis of pure silica zeolites in alkaline conditions.[9] The results, presented in Table 2,

Table 2. Transfer of Imidazolium Iodides from Water to Chloroform Solutions[a]

SDA	$(C+N)/q$[b]	% molar transfer
13DMI	7	22.50
123TMI	8	16.55
134TMI	8	28.78

[a]Following the experimental procedure in ref 9. [b]Ratio of carbon plus N atoms to charges in the cation.

indicate these imidazolium cations behave differently from the large series of organoammonium cations considered in the original report (containing the charged N in linear, cyclic, or polycyclic alkane moieties, but never in an aromatic ring).[9] There, hydrophobicity (or, more properly, the partitioning between water and cholorform) was found to be largely independent of the molecular geometry and shape or the nature (linear, cyclic, or polycyclic) and size of radicals bonded to N and mainly depended on the ratio between the total number of C atoms to charged N in each cation (C/N^+). Here we shall use the ratio of the total number of C and N atoms to the total number of cationic charges, $(C+N)/q$, for discussion, given the presence of two N atoms but a single charge in the imidazolium ring.

Results in Table 2 show that the molecular geometry has a notable influence on the hydrophobicity of the imidazolium cation, since 123TMI and 134TMI ($(C+N)/q$ = 8), despite being isomers, present a rather large difference in percentage of transfer to chloroform. Surprisingly, 123TMI shows the largest hydrophilicity of the three SDAs, despite the considerable acid character of the H at C2 in 13DMI and 134TMI. Additionally, the three imidazolium iodides show larger percentages of transfer to chloroform than the organoammonium iodides of similar size reported in the original work: tetramethyl- and tetraethylammonium iodides, with $(C+N)/q$ = 5 and 9, show no transfer to chloroform. The main difference between those

dx.doi.org/10.1021/ja209832y | J. Am. Chem.Soc. 2012, 134, 2255−2263

SDAs and our imidazolium cations is that in the latter the cationic charge resides on an aromatic ring (the imidazolium ring). Finally, we note that as the hydrophobicity increases, the efficiency of the imidazolium cations in directing the crystallization toward ITW decreases (see discussion below).

Characterization. Figure 1 shows the powder XRD patterns (obtained with a conventional low-resolution laboratory

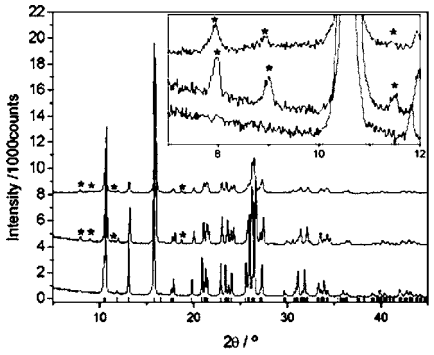

Figure 1. XRD powder patterns (laboratory data, *y*-offset for clarity) of as-made pure silica ITW zeolites prepared with (from bottom to top) 134-TMI, 13-DMI, and 123-TMI, with the low angle region shown in the inset (different *y*-offset). Vertical marks at the bottom are the allowed reflections in the originally reported *Cm* space group.[8] Asterisks mark extra reflections that revealed a doubling of the original cell.

diffractometer) of three as-made ITW zeolites synthesized using each one of the SDAs used in this work. While the three zeolites are easily recognized as belonging to the ITW framework type, it is clear that the samples prepared with 123TMI and 13DMI present four weak additional reflections that cannot be indexed in the originally reported *Cm* cell.[8] Both patterns were indexed using the program N-TREOR[24] implemented in Toby's CMPR toolkit,[25] revealing a doubling of the unit cell along *c*. Systematic absences were consistent with groups *I*2, *Im*, and *I*2/*m*.

This doubling of the unit cell is not an effect of the presence of organic or fluoride guests because the calcined materials also show the extra reflections, always with a weak intensity. In hindsight, very weak extra reflections (typically only the (−101) reflection of the double cell) may also be detected occasionally in calcined samples prepared using 134TMI and were previously mistaken as an MTT impurity. Apparently, preferred orientation effects, differences in crystal size and shape (see below), and XRD sample preparation or collection conditions likely cause some variability regarding the intensity of the extra reflections. FE-SEM images show that ITW crystallizes in the form of long and thin needles with very high aspect ratios when using 123TMI as SDA, while the use of 134TMI generally yield highly interpenetrated crystals with more similar dimensions in the three dimensions (Figure 2). In the case of 13DMI-ITW, we observed in the same sample crystals with two dimensions larger than the third one as well as oriented aggregates. This supports the idea that preferred orientation effects may be more pronounced with 123TMI and 13DMI than with 134TMI.

The ITW as-made zeolites prepared with the three SDAs contain close to four organic cations and four fluoride anions per 48 SiO_2 (i.e., per *I*2/*m* unit cell), as shown in Table 3. In the corresponding ^{19}F MAS NMR spectra (Figure S1), a sharp resonance around −40 ppm (−38.9, −40.1, and −40.3 ppm for 123TMI-, 134TMI-, and 13DMI-ITW, respectively) is a clear

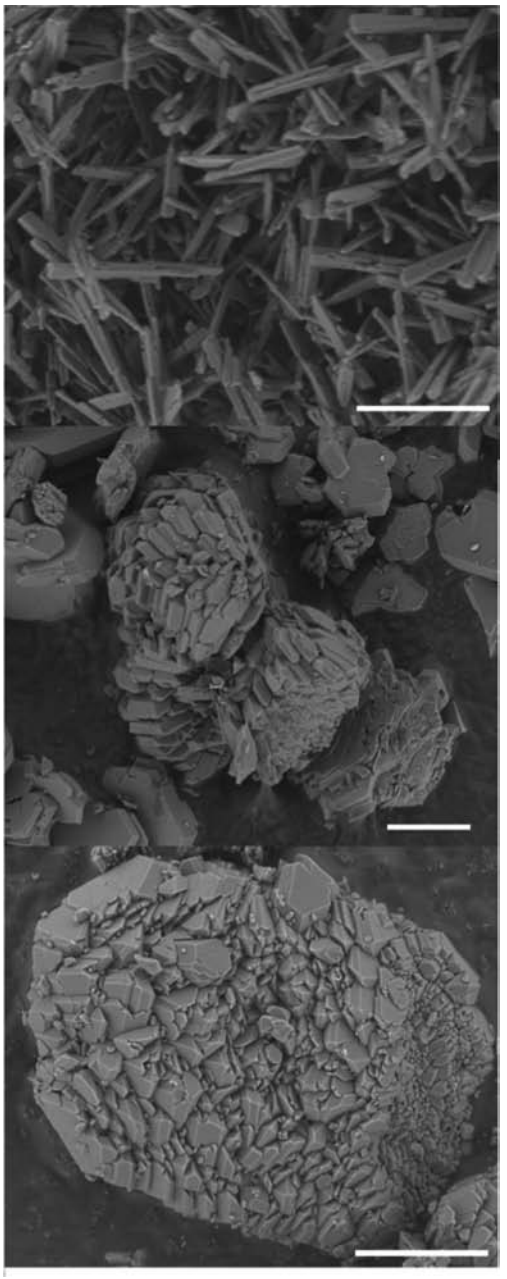

Figure 2. FE-SEM images of (from bottom to top, scale bars in parentheses): 134TMI-ITW (4 μm), 13DMI-ITW (5 μm), and 123TMI-ITW (2 μm).

fingerprint for fluoride occluded in the D4R silica cages.[26] On the other hand, the ^{13}C MAS NMR spectra (Figure S2) of the three materials indicate the SDAs are occluded essentially intact in the ITW framework, and, given its relatively large size, they must reside in the relatively large, slit-shaped [$4^4 5^4 6^4 8^4$] cavities. With regard to 13DMI-TON zeolite, it contains a smaller organic and fluoride content (Table 3), with the SDA occluded intact (^{13}C MAS NMR, Figure S2). The ^{19}F NMR resonance around −76.4 ppm (Figure S1) is in the typical range for fluoride occluded in silica zeolites with covalent bonding to Si and, in fact, is close to the resonance found in 134TMIF-SiO_2-TON (−77.6 ppm), suggesting here also that fluoride is bonded to framework silicon, yielding a pentacoordinated [$SiO_{4/2}F$]$^-$.[7] Nonetheless, no resonance assignable to direct Si−F bonds or connectivity defects are observed in the ^{29}Si MAS

dx.doi.org/10.1021/ja209832y | *J. Am. Chem.Soc.* 2012, 134, 2255−2263

Table 3. Unit Cell Compositions of the Synthesized Zeolites

	% weight found				% expected[b]			
	C	H	N	weight loss/%[a]	C	H	N	unit cell composition
134TMIITW	8.27	1.43	3.41	16.06 (15.42)	8.43	1.34	3.28	$\|C_6H_{11}N_2F|_2[SiO_2]_{24}$:0.39$H_2O$
123TMI-ITW	8.08	1.36	3.32	15.1 (14.99)	8.46	1.31	3.29	$\|C_6H_{11}N_2F|_4[SiO_2]_{48}$:0.18$H_2O$
13DMI-ITW	7.14	1.25	3.40	12.46 (14.10)	7.12	1.16	3.32	$\|C_5H_9N_2F|_4[SiO_2]_{48}$:1.36$H_2O$
13DMI-TON	3.00	0.57	1.31	7.51 (6.93)	2.84	0.53	1.32	$\|C_5H_9N_2F|_{0.73}[SiO_2]_{24}$:0.73$H_2O$

[a]Experimental thermogravimetric weight loss up to 980 °C (in parentheses, expected for the composition given in the last column). [b]For the composition given in the last column.

NMR spectrum (Figure 3, bottom trace). ^{29}Si MAS NMR of the three as-made ITW materials reveal, in addition to a lack of any significant concentration of Q3 connectivity defects in the samples (region around −101 ppm), significant resolution of crystallographic sites in tetrahedral coordination, with no signs of pentacoordinated units (region around −145 ppm) or of Si sites changing coordination between 4 and 5 (region between −120 and −150 ppm)[27] (Figure 3). This is the typical situation when F is occluded in siliceous D4R units. But there is also a large difference between the sample crystallized with 134TMI, showing only two intense resonances, and the ones prepared with 123TMI and 13DMI, which present a higher resolution of crystallographic sites, with up to five resonances, and have a lower overall intensity. Increasing the delay time between cycles from 60 to 180 s did not change appreciably the relative intensities of different resonances within each spectrum, nor the noted differences in overall intensity among samples.

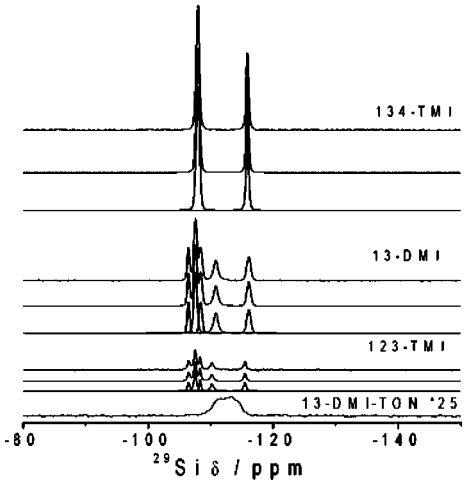

Figure 3. ^{29}Si MAS NMR spectra of as-made (from bottom to top) 13DMI-TON, 123TMI-ITW, 13DMI-ITW, and 134TMI-ITW zeolites. The recycle delay time was 60 s for the TON spectrum and 180 s for the ITW spectra. For each ITW sample the experimental, simulated, and deconvoluted components (from top to bottom) are shown. Differences in the absolute intensities for each sample are attributed to large differences in their packing inside the RMN rotor.

The intensity differences are thus much likely due to the very different packing inside the rotor than can be achieved with each type of sample, due to their largely different crystal size and morphology (Figure 2). In contrast to the as-made samples, the three calcined materials show very similar spectra in terms of number, intensity, and chemical shifts of the resonances, irrespective of the SDA used, as expected for isostructural materials with the same chemical composition, but they still show similar differences in overall intensity (Figure S3).

Structure Analysis. The evidence for cell doubling in 123TMI-ITW and 13DMI-ITW and the differences observed in the ^{29}Si MAS NMR spectra of these materials with respect to that of 134TMI-ITW prompted a structural investigation of these materials, which was also motivated by the interest in determining the approximate location and orientation of the SDA cations and to shed light on structure/synthesis relationships. A calcined ITW that also presents the extra reflections (prepared with 123TMI) was also included in the study. Details of the analyses, including Rietveld plots (Figures S4−S6), crystallographic and experimental parameters (Table S1), and the crystallographic data in CIF format, can be found in the Supporting Information.

The location of guests in 123TMI-ITW and 13DMI-ITW, found by Fourier analysis (see Supporting Information), is similar to that found in 134TMI-ITW:[8] fluoride always resides in D4R units, while the organic cations were found in the larger $[4^45^46^48^4]$ obloid cavity, with the imidazolium ring in the equatorial plane of the cage (Figure 4). In 123TMI-ITW (see Supporting Information), the orientation initially found by Fourier analysis had the methyl groups in positions 1 and 3

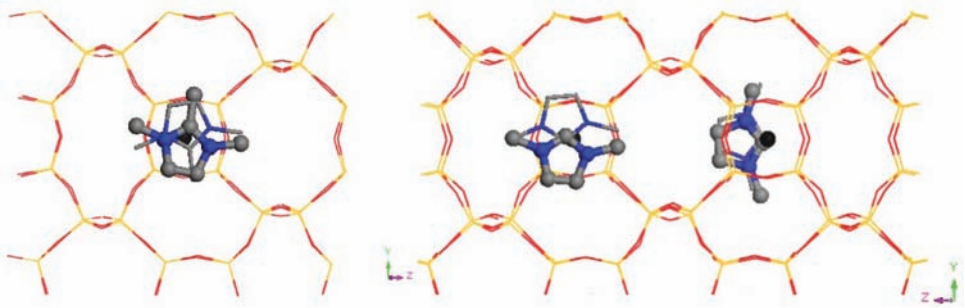

Figure 4. Location of 123TMI (left) and 13DMI (right) in as-made ITW, as found by Fourier analysis and Rietveld refinement. For 123TMI-ITW, only half a unit cell with the most preferred orientation is shown. For clarity, two symmetrical positions of each cation are shown, one as ball and sticks, and the other drawn as lines. Si, yellow; O, red; N, blue; C, gray; and F, black.

dx.doi.org/10.1021/ja209832y | J. Am. Chem.Soc. 2012, 134, 2255−2263

Table 4. Unit Cell Parameters of ITW Zeolites

	calcined 123TMI-ITW	as-made 123TMI-ITW	as-made 13DMI-ITW	as-made 134TMI-ITW[a]
space group	*I*2/*m*	*I*2/*m*	*I*/2*m*	*Cm*
a/Å	10.32658(10)	10.43748(9)	10.42127(27)	10.4478(3)
b/Å	14.99940(13)	14.80768(15)	14.8998(4)	14.9854(4)
c/Å	17.71021(19)	17.50255(18)	17.5897(5)	8.8366(3)
β/°	105.3959(7)	106.0895(7)	105.8066(13)	105.935(2)
cell volume/Å^3	2644.74(5)	2599.15(5)	2627.97(18)	1330.34(7)
calc density/g cm^{-3}	1.81	2.14	1.97	2.12
FD/Si per nm^3	18.15	18.47	18.27	18.04

[a]From ref 8.

facing the 8MR windows and that in position 2 up or down slightly off [010]. However, from preliminary theoretical calculations a second orientation could also exist, with the methyl groups in positions 1 and 3 pointing up and down the [010] axis and that in position 2 pointing to the 8MR windows (Figure 4, left). This orientation was also introduced, and the relative occupancies were refined, finally yielding the first orientation commented above as the most favorable one (in a 75:25 ratio). The center of gravity of the cation is very close to the center of the cavity at (0.5, 0, 0.25) for both orientations: 0.28 and 0.27 Å respectively for the first and second orientations commented above. Cations in the most populated orientation and with the same alignment in adjacent cavities have slightly short methyl−methyl distances of 3.96 Å, which may suggest alternation of up and down alignments (yielding methyl−methyl distances of 4.09 Å).

For 13DMI-ITW, after refining the position and orientation of a single cation (with one methyl pointing up or down slightly off [010] and the other one pointing to the 8MR window), substantial residual electronic density remaining inside the cage suggested the need for a second one (see details in Supporting Information) to describe disorder within the cage. In the final structure, one cation has the methyl groups up and down [010], while in the other they point to the 8MR windows, and both have approximately the same occupancy (Figure 4, right). The center of gravity is close to the cavity center (0.55 Å) for the first orientation mentioned and is farther apart (1.12. Å) for the second one. For this orientation, short methyl−methyl distances of 3.12 Å between cations in adjacent cavities may be avoided by alternation of both orientations.

With regard to the SiO_2 framework itself, for the three *I*2/*m* structures reported here (as-made and calcined 123TMI-ITW and as-made 13DMI-ITW), the pores along [100], while topologically identical, present two actual configurations alternating along [001]: one is elongated and has a very small aperture (2.2 × 4.5 Å in the calcined structure), while the second is more circular and open (3.1 × 3.8 Å). This is clearly observed for 123TMI-ITW and 13DMI-ITW in Figure 4. The pore along [001] is more uniform, with pore dimensions 3.8 × 3.9 Å in the calcined materials. For comparison, the reported *Cm* structure of calcined SiO_2-ITW showed pores of 2.4 × 5.3 Å and 3.8 × 4.1 Å along [100] and [001], respectively.

The striking differences between the ^{29}Si MAS NMR spectra of the as-made ITW samples commented above can be understood by considering the average SiOSi angles of each Si site in each of these structures (Table S2). In all cases, Si sites involved in D4R rings (which are two-thirds of the total Si sites) show significantly smaller SiOSi angles, resulting in chemical shifts at considerably lower fields, than Si sites not involved in D4R. In the reported *Cm* structure of 134TMI-ITW, the average SiOSi angles of the six Si sites, all with the same multiplicity, are closely grouped around two values: the four Si sites making the D4R have more acute average angles (142.9 ± 2.7°) than the other two sites (155.5 ± 2.1°).[8] In our refined structures of 123TMI-ITW and 13DMI-ITW, the average SiOSi angles are significantly more spread, with non-D4R sites having angles of 151.1 ± 3.7° and 152.4 ± 3.5°, respectively, and D4R sites having angles of 140.3 ± 5.2° and 142.3 ± 3.7°, respectively. This results in a wider range of chemical shifts and a larger resolution of crystallographic sites in the ^{29}Si MAS NMR spectra. It is, however, still evident that Si sites belonging to D4R units have average SiOSi angles far more acute than non-D4R sites. The ^{29}Si chemical shifts calculated from the average angles using the equation of Thomas et al.[28] agree reasonably well with the experimental values, with disagreements generally smaller than 1 or 2 ppm (Table S2).

Table 4 collects cell parameters for as-made and calcined ITW samples. We note that the order of decreasing FD for the three imidazolium-ITW zeolites parallels the order of efficient SDA activity of the imidazolium cations, as 123TMI-ITW has a larger FD than 13DMI-ITW, which has also a larger FD than 134TMI-ITW (Table 4). Although drawing conclusions from this kind of observations may be considered generally too daring in zeolites, we also note that upon calcination 123TMI-ITW and 13DMI-ITW expand their cell volumes by 1.8 and 0.6%. Furthermore, calcination of all the three imidazolium-containing ITW zeolites produces a shortening of the *a* edge and *β* angle and an enlargement of the *b* and *c* edges. Considering that the [100] crystallographic axis is almost normal to the equatorial plane of the cavity and hence to the imidazolium plane, and that the shortest anion−cation distances (hence, the tightest anion−cation packing) occur approximately along this direction, we think its shortening upon calcination is relevant and suggests, as previously claimed for 134TMI-ITW,[8] the cation is "pushing" the cavity walls outward. With the *a* parameter larger in the as-made than in the calcined materials, the volume shrinkage noted above becomes even more remarkable and may suggest a stronger host−guest interaction in 123TMI-ITW, possibly enabled by its larger ionization (see below). The thickness of the cavity, measured as the shortest distance from an O in D4R to an O in the next D4R along [100], is 3.67, 3.77, 3.85, and 3.95 Å in calcined SiO_2-ITW, 123TMI-ITW, 13DMI-ITW, and 134TMI-ITW, respectively, suggesting the anion−cation packing along [100] decreases in the order 123TMI-ITW >13DMI-ITW > 134TMI-ITW, again paralleling the order of efficiency of the corresponding cations.

Calculations. *Model Structures.* In a previous work, the geometries and energies of 134TMIF-SiO_2 in TON and ITW frameworks have been reported at the same calculation level as

dx.doi.org/10.1021/ja209832y | J. Am. Chem.Soc. 2012, 134, 2255−2263

mentioned in the previous section.[7] In the present calculations concerning ITW framework with occluded species, the corresponding SDAs and F^- were initially located inside the obloid cavity and D4R unit, respectively. In all ITW structures, the primitive cell in space group *P*1 has been considered for calculations. As concerns the TON framework, the SDAs were located in a supercell model duplicated with respect to the original crystal along the lattice direction parallel to the 10-ring channel. The F^-, at time, was initially located near one of the eight symmetry-equivalent Si(3) which is in the closest position to the SDA. This procedure mimics the one previously followed for 134TMIF-SiO_2-TON.[7] The full sets of structural data of 123TMI-XXX and 13DMIF-XXX (XXX = TON, ITW) are summarized in Tables S3−S8 in the Supporting Information. These include alternate orientations for the SDA inside the ITW cavity, which were found to be slightly less stable but nonetheless feasible, in agreement with the structural refinements discussed above.

In the previously mentioned work,[7] the optimized geometry of 134TMIF-ITW was reported with the methyl groups on the channel axis for that in position 4 and out of it for those in 1 and 3. In the present work, the methyl group at position 2 of the imidazolium ring is oriented along the [110] direction of the primitive cell in 123TMI-ITW. The 13DMI molecule is oriented with the position 2 of the ring along the [001] direction. The center of mass of both SDAs is close to the center of the 4MR. The accommodation of both SDAs within the ITW framework is shown in Figure S7 of the Supporting Information. As in the case of 134TMIF-ITW,[7,13] the F^- is placed close to the center of the D4R unit in 123TMIF-ITW and 13DMIF-ITW, and as a consequence of the orientation of the SDA inside the cavity, the distances of N atoms to F^- are very similar in the three systems, as it is reported in Table S9, where only the closest N−F distances are listed. It is important to note that distances and angles listed in Table S9 are those related to the Si and O atoms of the D4R units which are closest to the F^- and imidazolium fragments, respectively. As it is reckoned in the table, Si−O distances do not differ from those of the clean ITW framework, while there is an increment on O−Si−O angles and decreasing on Si−O−Si ones. These distortions of D4R units are a consequence of the presence of F^- inside them.

As concerns the optimized 123TMIF-TON and 13DMIF-TON models, a distortion of the tetrahedral conformation around one Si atom toward a trigonal bipyramid is observed as a consequence of the presence of F^- in the framework. As in the case of 134TMIF-TON,[7] the principal axis is determined by the F, O(4b), and Si(3) atoms, while the remaining O atoms roughly lie on a close to perpendicular plane. In Table S10 some selected distances and angles are reported, which correspond to the optimized TON structures. The main evidence of the distortion to a trigonal bipyramidal accommodation are the very similar Si(3)−O(4b) and Si(3)−F distances, and the O−Si−O(4b) angles which approach 90°. Meanwhile, the O(4b)−Si(3)−F angles have values of almost 180° in the three systems with occluded species.

The orientations of the different imidazolium cations inside the 10-ring channel of the TON framework in the optimized geometries are represented in Figure S8. When 123TMI is occluded in TON, two of the methyl groups (positions 1 and 3) are along the channel direction, while the third one (position 2) is out of it and close to the channel wall. In fact, the oxygen atoms involved in the OH closest distances of the three systems, listed in Table S10, correspond to those located over the principal axis of the trigonal bipyramidal conformation mentioned above; in turn, the H is bonded to a ring atom in 134TMI and 13DMI, while in 123TMI it belongs to the central methyl group.

Relative Stabilities. To make a comparison among the relative stabilities of the materials with occluded species, the ΔE of three hypothetical reactions representing the exchange of $SDA^+ + F^-$ between TON and ITW frameworks were calculated from the values reported in Table S11, according to the following exchange reaction between SiO2-ITW and SiO2-TON used here to quantify the relative stability of the as-made zeolites:

$$\mathrm{SDAF}[(\mathrm{SiO_2})_{12}\text{-TON}]_2 + (\mathrm{SiO_2})_{12}\text{-ITW} \rightarrow \mathrm{SDAF}\text{-}(\mathrm{SiO_2})_{12}\text{-ITW} + 2[(\mathrm{SiO_2})_{12}\text{-TON}] \quad (\mathrm{SDA} = 134\mathrm{TMI},\ 13\mathrm{DMI},\ 123\mathrm{TMI}) \quad (1)$$

where the composition of the primitive cell of the corresponding pure silica framework is indicated in parentheses.

In all cases, as shown in Table 5, it turns out that the ITW silica with occluded species is more stable than the equivalent compound with TON SiO_2. Moreover, this stability difference is higher by more than 40 kJ/mol in the case of occluded 123TMI.

Table 5. Summary of Calculated Data for Optimized As-Made SiO_2-ITW Structures[a]

			average Born charges, $\langle q \rangle$[c]	
SDA	ΔE/kJ mol^{-1}	ΔT/°	Si	O
134TMIF[b]	−38.2	3.68	3.36402	−1.69164
123TMIF	−88.0	3.76	3.38419	−1.70258
13DMIF	−42.0	3.70	3.36849	−1.69296
no SDA			3.26101	−1.6305

[a]Relative stability (ΔE) and deviation from regularity of tetrahedra (ΔT) are defined in the text. [b]ΔE and ΔT from ref 7. [c]Born charges are averaged along all Si and O atoms of the systems.

The stability trend, according to eq 1, of the as-made species shown in Table 5 has a net correlation with other microscopic properties. The calculated standard deviation from regularity (OTO angle 109.47°) of the SiO_4 tetrahedra, and the Born charges averaged over Si and O atoms are also listed in columns 2−4 of the same table. The former is a quantity directly related to the directionality of the Si−O bonds, and indirectly to their degree of covalency, as the bond-directionality toward the vertices of a regular SiO_4 tetrahedron is currently attributed to the semi-covalent character of the bonding between Si sp^3 and O electrons. As previously discussed,[7] the ability of these primary tetrahedral units to distort themselves so as to adapt to the quite tense D4R accommodation, is a crucial effect that allows the ITW framework to crystallize against the tendency toward the formation of the denser and less strained SiO_2-TON. According to the results shown in Table 5, the largest stability of the 123TMI-ITW is associated with the largest distortion from regularity of the tetrahedra, indicating that the influence of the SDA favors in this case the structural relaxation of the silica moiety. It turns out that, to a lower extent, a similar effect is occurring with the other SDAs, the as-made material synthesized with 134TMI, the originally reported SDA for ITW, being the least flexible and least stable one.[14] The loss of rigidity in

dx.doi.org/10.1021/ja209832y | J. Am. Chem.Soc. 2012, 134, 2255−2263

the SiO_4 units allows the structure to contract in volume (trying to maximally fill the void spaces and to maximize contacts between SDA and silica skeleton), and comparison between relative stabilities and densities in Tables 5 and 4, respectively, shows that for the as-made ITW materials, the more stable, the denser.

On the other hand, the average Born charges reported in Table 5 allow us to interpret the previous results in terms of polarization and degree of ionicity of the Si−O bond. As already observed previously,[7,13] the charge separation between framework O and Si atoms increases substantially when the SDA and the F^- are occluded inside the material cavities. This is apparent from the Born charge-difference distribution shown in Figure 9S. The charge-difference distribution is more localized in the case of TON with occluded species (on Si(3), to which the F^- is coordinated, and neighboring O atoms), compared to the more sparse charges of Si and O atoms in SDA-ITW zeolites (all of them belonging to the D4R unit around the occluded F^-). Nevertheless, the ionicity displays slight but net differences with the SDA nature, showing a clear correspondence with relative stabilities and deviation from regularity of the SiO_4 tetrahedra. It turns out that the larger the charge separation is, the more stable is the ITW with respect to TON as-made materials and the more irregular are the tetrahedra of the ITW silica moiety. In other words, the loss of directionality of the Si−O bond, attributable to a less covalent character of the interaction, is associated to a charge increment that would consistently indicate an enhanced ionicity of the silica moiety, leading to more flexible and stable as-made SiO_2 zeolites.

Finally, we next shall consider SDA features typically used to rationalize structure-direction in the synthesis of zeolites (size, shape, hydrophilicity, conformational rigidity).[3,4,9,23] The three SDAs show a similar conformational flexibility, restricted to the rotation of the methyl groups along C−N or C−C bonds. The 123TMI and 134TMI isomers have a similar molecular volume, which is slightly smaller in the case of 13DMI. The shape is dominated by the flat, thin, and planar imidazolium ring, with methyl groups pointing outward. In view of the different orientations found inside the cavity, the relative position of different methyl groups in the imidazolium ring may not pose significant differences among the three cations inside the cage: in all the three zeolites the methyl groups, in one or another of the orientations found, point approximately in the direction of the pore and up and down the [010] axis . In addition, we have found notable differences in the hydrophobic character among the three SDAs (Table 2). Remarkably, the order of decreasing hydrophobicity follows the order of increasing stabilization of the ITW framework, suggesting hydrophobicity may be the main difference between these cations that can be related to their performance as SDAs. As we have previously shown for 134TMI-ITW and show now also for 123TMI-ITW and 13DMI-ITW, the stabilization of the strained ITW framework critically depends on the ionization, or decreased covalent character, of the Si−O bond through host−guest interactions. Thus, the less hydrophobic character of 123TMI may indicate that a larger hydrophilicity affords a larger ionization and stabilization of the ITW framework.

It is thus tempting to consider the silica framework as a "solid solvent", in which a sort of polarity affinity, similar to that holding in liquid solutions, makes the SiO_2 host to increase its bond polarization as the SDA becomes more and more hydrophilic. Nonetheless, there is presently a lack of precise theoretical support for this notion. In this respect, we note that the hydrophobic character of organic cations may have a different impact in fluoride vs hydroxide synthesis routes, due to the different host−guest interactions and, particularly, the likely differences in the localization of the anionic charge in the silica framework, in view of the global polarization effects that may be achieved in silica zeolites with fluoride occluded in D4R. Thus, general conclusions regarding one route should not be straightforwardly generalized to the other.

■ CONCLUSIONS

Three small methylimidazolium cations are shown to be capable of producing pure silica ITW zeolite. Two of them can also produce zeolite TON, but this transforms *in situ* into ITW. While the system follows the Villaescusa rule in that lower framework density phases are favored at high concentration conditions, our observations invalidate a supersaturation hypothesis previously proposed:[16] the phase favored at higher concentration is in this case the thermodynamically more stable one.

DFT calculations agree well with the experimental observations and provide a strong support to the idea that host−guest interactions may afford a decreased covalency of the Si−O bond that appears to be central to structure-direction in the synthesis of zeolites with strained silica frameworks. This decreased covalency is supported by the increased polarity of the framework, as derived from the Born charges analysis and deviation from tetrahedrality. As a matter of fact, a clear correlation appears between the decrease in the covalency of the silica moiety, density increase, and better packing along the[100] direction in the as-made materials, as the SDA becomes more hydrophilic. While there is no clear theoretical background to relate this effect, we consider very striking the coincidence between hydrophilic nature of the cation and decreased covalency.

■ ASSOCIATED CONTENT

Ⓢ Supporting Information

Details of multinuclear MAS NMR, ^{13}C, ^{19}F, and ^{29}Si spectra, details of Rietveld refinements, Rietveld plots, crystallographic and structural parameters for as-made and calcined 123TMI-ITW and as-made 13DMI-ITW (full crystallographic data also provided as CIF files), structural data for the optimized SDA-ITW and SDA-TON structures, images of the relevant orientation of the SDA in both zeolites, and total energies of the optimized structures. This material is available free of charge via the Internet at http://pubs.acs.org.

■ AUTHOR INFORMATION

Corresponding Author

macamblor@icmm.csic.es

■ ACKNOWLEDGMENTS

Financial support by the Spanish CICYT (project MAT2009-09960) is gratefully acknowledged. We warmly thank Prof. S. B. Hong (POSTECH) for sharing synchrotron beam time and Mr. J. Shin for collecting the powder XRD data at Pohang Accelerator Laboratory (Pohang, Korea). We thank A. Valera for technical expertise (FE-SEM). A.R. acknowledges a JAE fellowship from CSIC and Fondo Social Europeo from EU. E.M.-M. thanks Mexican PROMEP for a postdoctoral fellowship.

REFERENCES

(1) Baerlocher Ch.; McCusker, L. B. Database of Zeolite Structures: http://www.iza-structure.org/databases/

(2) Lobo, R. F.; Pan, M.; Chan, I.; Medrud, R. C.; Zones, S. I.; Crozier, P. A.; Davis, M. E. *J. Phys. Chem.* **1994**, *98*, 12040. Lobo, R. F.; Pan, M.; Chan, I.; Li, H. X.; Medrud, R. C.; Zones, S. I.; Crozier, P. A.; Davis, M. E. *Science* **1993**, *262*, 1543.

(3) Gies, H.; Marler, B. *Zeolites* **1992**, *12*, 42. Gies, H.; Marler, B.; Werthmann, U. In *Molecular sieves—Science and technology*; Weitkamp, J., Karge, H. G., Eds.; Springer: Berlin, 1998; p 35.

(4) Davis, M. E.; Zones, S. I. In *Synthesis of Porous Materials*; Occelli, M. L., Kessler, H., Eds.; Marcel Dekker: NewYork, 1997; p 1. Zones, S. I.; Nakagawa, Y.; Lee, G. S.; Chen, C. Y.; Yuen, L. T. *Microporous Mesoporous Mater.* **1998**, *21*, 199. Lobo, R. F.; Zones, S. I.; Davis, M. E. *J. Incl. Phenom. Mol. Recognit.* **1995**, *21*, 47. Zones, S. I.; Olmstead, M. M.; Santilli, D. S. *J. Am. Chem. Soc.* **1992**, *114*, 4195. Zones, S. I.; Nakagawa, Y.; Yuen, L. T.; Harris, T. V. *J. Am. Chem. Soc.* **1996**, *118*, 7558. Zones, S. I. *Microporous Mater.* **1994**, *2*, 281. Nakagawa, Y.; Lee, G. S.; Harris, T. V.; Yuen, L. T.; Zones, S. I. *Microporous Mesoporous Mater.* **1998**, *22*, 69. Wagner, P.; Nakagawa, Y.; Lee, G. S.; Davis, M. E.; Elomari, S.; Medrud, R. C.; Zones, S. I. *J. Am. Chem. Soc.* **2000**, *122*, 263.

(5) Villaescusa, L. A.; Camblor, M. A. *Rec. Res. Dev. Chem.* **2003**, *1*, 93.

(6) Piccione, P. M.; Laberty, C.; Yang, S.; Camblor, M. A.; Navrotsky, A.; Davis, M. E. *J. Phys. Chem. B* **2000**, *104*, 10001.

(7) Zicovich-Wilson, C. M.; Gándara, F.; Monge, A.; Camblor, M. A. *J. Am. Chem. Soc.* **2010**, *132*, 3461.

(8) Yang, X.; Camblor, M. A.; Lee, Y.; Liu, H.; Olson, D. H. *J. Am. Chem. Soc.* **2004**, *126*, 10403.

(9) Kubota, Y.; Helmkamp, M. M.; Zones, S. I.; Davis, M. E. *Microporous Mater.* **1996**, *6*, 213.

(10) Becke, A. D. *J. Chem. Phys.* **1993**, *98*, 5648.

(11) Lee, C.; Yang, W.; Parr, R. G. *Phys. Rev. B* **1988**, *37*, 785.

(12) Dovesi, R.; Saunders, V. R.; Roetti, C.; Orlando, R.; Zicovich-Wilson, C. M.; Pascale, F.; Civalleri, B.; Doll, K.; Harrison, N. M.; Bush, I. J.; D'Arco, P.; Llunell, M. CRYSTAL09 Users Manual, University of Turin, 2009, Turin; available online at http://www.crystal.unito.it.

(13) Zicovich-Wilson, C. M.; San-Román, M. L.; Camblor, M. A.; Pascale, F.; Durand-Niconoff, J. S. *J. Am. Chem. Soc.* **2007**, *129*, 11512.

(14) Barrett, P. A.; Boix, T.; Puche, M.; Olson, D. H.; Jordan, E.; Koller, H.; Camblor, M. A. *Chem. Commun.* **2003**, 2114.

(15) Camblor, M. A.; Hong, S. B. In *Porous Materials*; Bruce, D. W., O'Hare, D., Walton, R. I., Eds.; Wiley: Chichester, 2011; p 265.

(16) Camblor, M. A.; Villaescusa, L. A.; Díaz-Cabañas, M. J. *Top. Catal.* **1999**, *9*, 59.

(17) Arranz, M.; Pérez-Pariente, J.; Wright, P. A.; Slawin, A. M. Z.; Blasco, T.; Gómez-Hortigüela, L.; Corà, F. *Chem. Mater.* **2005**, *17*, 4374. Zones, S. I.; Darton, R. J.; Morris, R.; Hwang, S. J. *J. Phys. Chem. B* **2005**, *109*, 652. Zones, S. I.; Hwang, S. J.; Elomari, S.; Ogino, I.; Davis, M. E.; Burton, A. W. *C.R. Chimie* **2005**, *8*, 267. Burton, A. W.; Lee, G. S.; Zones, S. I. *Microporous Mesoporous Mater.* **2006**, *90*, 129. Zones, S. I.; Burton, A. W.; Lee, G. S.; Olmstead, M. M. *J. Am. Chem. Soc.* **2007**, *129*, 9066.

(18) Zones, S. I. *Zeolites* **1989**, *9*, 458.

(19) Zones, S. I.; Burton, A. W. *J. Mater. Chem.* **2005**, *15*, 4215.

(20) Caullet, P.; Guth, J. L.; Hazm, J.; Lamblin, J. M.; Gies, H. *Eur. J. Solid State Inorg. Chem.* **1991**, *28*, 345.

(21) Guth, J. L.; Kessler, H.; Caullet, P.; Hazm, J.; Merrouche, A.; Patarin, J. In *Proceedings of the 9th International Zeolite Conference*; von Ballmoos, R., Higgins, J. B., Treacy, M. M. J., Eds.; Butterworth-Heinemann: 1993; p 215.

(22) Archer, R. H.; Zones, S. I.; Davis, M. E. *Microporous Mesoporous Mater.* **2010**, *130*, 255.

(23) Goretsky, A. V.; Beck, L. W.; Zones, S. I.; Davis, M. E. *Microporous Mesoporous Mater.* **1999**, *28*, 387.

(24) Werner, P.-E.; Eriksson, L.; Westdahl, M. *J. Appl. Crystallogr.* **1985**, *18*, 367.

(25) Toby, B. H. *J. Appl. Crystallogr.* **2005**, *38*, 1040.

(26) Camblor, M. A.; Barrett, P. A.; Díaz-Cabañas, M. J.; Villaescusa, L. A.; Puche, M.; Boix, T.; Pérez, E.; Koller, H. *Microporous Mesoporous Mater.* **2001**, *48*, 11.

(27) Koller, H.; Wölker, A.; Villaescusa, L. A.; Díaz-Cabañas, M. J.; Valencia, S.; Camblor, M. A. *J. Am. Chem. Soc.* **1999**, *121*, 3368.

(28) Thomas, J. M.; Klinowski, J.; Ramdas, S.; Hunter, B. K.; Tennakoon, D. T. B. *Chem. Phys. Lett.* **1983**, *102*, 158.